Experimental Investigation of Mode II Fracture Properties of Parallel Strand Bamboo Composite by End Notched Flexure Test

Xiaorui Wang,[a,b,c] Aiping Zhou,[a,b,*] and Ying Hei Chui [d]

Parallel strand bamboo (PSB) is a high-strength bamboo composite that has been used in construction in recent years. Crack growth is a major concern in the design of PSB components for building structures. This study investigated the mode II fracture properties of PSB composite under in-plane shear action, starting from the end notched flexure (ENF) test as the prototype of specimens. The compliance based beam method (CBBM) was used to analyze the crack propagation process. The results showed that crack propagation of mode II fracture of PSB was self-similar cracking with cracks parallel to the strand. The fracture process contained two stages: the development of the Fracture Process Zone (FPZ) and the crack propagation stage. The critical energy release rate G_{IIc} was a constant independent of the initial crack length, with a mean value of 2.61 N/mm; the mean value of fracture toughness K_{IIc} was 4436 $kN \cdot m^{-3/2}$, which is greater than those of commonly used timber products. The R-curve showed a gradual increase before crack extension due to the development of the FPZ but became approximately horizontal during crack propagation.

Keywords: Parallel strand bamboo; Mode II fracture; ENF test; Energy release rate; R-curve; Fracture toughness

*Contact information: a: National Engineering Research Center of Biomaterials, Nanjing Forestry University, 159 Longpan Road, Nanjing, China, 210037; b: College of Civil Engineering, Nanjing Forestry University, 159 Longpan Road, Nanjing, China, 210037; c: Faculty of Forestry and Environmental Management, University of New Brunswick, Fredericton, New Brunswick, Canada, E3B 5A3; d: Department of Civil and Environmental Engineering, University of Alberta, 116 St. and 85 Ave., Edmonton, Alberta, Canada, T6G 2R3; *Corresponding author: zaping2007@163.com*

INTRODUCTION

Parallel strand bamboo (PSB) is a bio-composite material manufactured by gluing bamboo strands with resin under high pressure, with superior attributes relative to those of wood products (Huang *et al*. 2015a). Because the bamboo strands are aligned in the longitudinal direction and are uniformly arranged in transverse direction, the gradient distribution of raw bamboo is eliminated. Therefore, PSB can be reasonably treated as an orthotropic composite. Parallel strand bamboo components are highly suitable for construction due to their outstanding mechanical properties (Huang *et al*. 2013, 2015b).

Because original gaps between the interfaces of strands or fibers cannot be absolutely avoided in manufacturing, microvoids are left and randomly scattered in PSB composites. Once a PSB component is subjected to loading action, these microvoids will extend and coalesce to form cracks due to the stress concentration around these microcracks. Experimental investigation has demonstrated that the decrease in strength of PSB components is commonly caused by fiber failure and inter-fiber matrix failure (Huang *et al*. 2015a). For wood-like composites such as PSB, the strength of fibers is

much higher than that of the matrix; hence, cracks usually propagate along the longitudinal direction and cause mode I, mode II, or mixed-mode cracks. When PSB components are subjected to bending action, shear failure may occur in the direction parallel to strands due to original crack extension in the region with high shear stress. In this situation, crack propagation takes place earlier than flexural failure; consequently, the ultimate load-carrying capacities of PSB bending components are sometimes controlled by mode II fracture toughness rather than bending strength. Therefore, fracture properties under in-plane shear action are critical in the design of PSB components for building structures.

As stated above, PSB composite is a wood-like, orthotropic composite, so the research methods of mode II fracture of wood and fibrous composites can be used as references. The short beam shear (SBS) test method (ASTM D2344 (2016)) was perhaps the first quality control test method used to investigate mode II fracture of composite materials. However, this method is more suitable for measuring the apparent interlaminar shear strength rather than mode II fracture toughness. The end notched flexure (ENF) test method is the most commonly used method to investigate mode II fracture energy release rate of composites (Barrett and Foschi 1977; Russell and Street 1982; Carlsson *et al*. 1986; Wang and Williams 1992; Corleto and Hogan 1995; Williams and Hadavinia 2002). The geometry of the ENF specimen is essentially a three-point flexure specimen with an embedded through-width notch placed at the mid-surface (ASTM D7905 (2014)). Barrett and Foschi (1977) were the earliest to utilize the ENF specimen to characterize the mode II fracture of wood. Russell and Street (1982) used the ENF specimen to characterize mode II critical energy release rate of advanced composites based on elementary beam theory. Subsequently, a development of the ENF test method was proposed by Carlsson *et al*. (1986), who calculated the displacement caused by shearing force in ENF specimen based on Timoshenko's beam theory. Several researchers (Wang and Williams 1992; Corleto and Hogan 1995; Williams and Hadavinia 2002) derived the crack tip deformation as a correction of crack length in ENF specimen. At this point, the ENF test method for mode II fracture was basically improved. Recently, Valvo (2018) presented a critical review of the relevant literature on mode II fracture starting from the ENF test, and theoretically investigated the effects of shear on mode II delamination. Several extensions of mode II fracture flexural specimens have been proposed since the introduction of the ENF specimen. For example, Wang and Vu Khanh (1996) introduced end loaded split (ELS) tests. However, the usage of the ELS specimen is limited by large displacement at the loading point. These flexural specimens are all similar to the ENF specimen in geometry. The specimen of the ENF test is easy to manufacture, the test configuration is simple, and the data-reduction methodology is straightforward. The most attractive feature of the ENF test is that it particularly suits testing for quasi-brittle materials like wood or bamboo composites. For these reasons, the ENF test was used to characterize the mode II fracture of PSB composites in this study.

EXPERIMENTAL

Theory

As shown in Fig. 1, an ENF specimen with an initial crack, a, is loaded by P at mid-span; the coordinate system is set up as shown. The compliance, C, at the loading point is given as follows,

$$C = \frac{\delta}{P} = \frac{2L^3 + 3a^3}{12EI} + \frac{3L}{5GA} \quad (1)$$

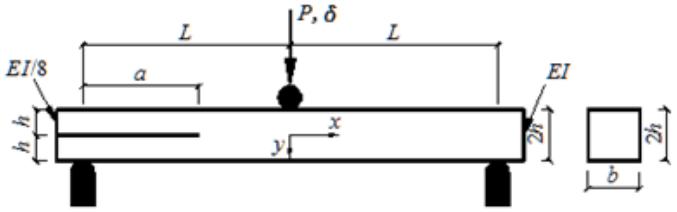

Fig. 1. ENF test

where P (N) is the applied load, δ (mm) is the loading point displacement, E (MPa) is Young's modulus in the longitudinal axis, I (mm^4) is the second moment of cross-sectional area in the crack-free region, A (mm^2) is the cross-sectional area of the crack-free region, G (MPa) is the shear modulus in the length-depth plane, and [3L/(5GA)] is the displacement caused by shear stress. Based on Griffith theory (Griffith 1921; Irwin 1956), the energy release rate can be expressed as,

$$G_{II} = \frac{P^2}{2b}\frac{dC}{da} = \frac{3a^2P^2}{8EIb} \quad (2)$$

where b (mm) is the specimen width, and a (mm) is the crack length. The critical energy release rate, G_{IIc}, can be calculated by replacing P with P_c, the critical load at crack initiation.

Due to the plastic deformation at the crack tip, the G_{IIc} values are usually underestimated by using Eq. 2 directly. Therefore, the equivalent crack length, a_{eq}, was introduced in the compliance based beam method (CBBM) to replace a in Eq. 2 (De Moura *et al.* 2006; De Moura *et al.* 2009). The equivalent crack length is given as follows,

$$a_{eq} = \left[\frac{C_{corr}}{C_{0corr}}a^3 + \frac{2}{3}\left(\frac{C_{corr}}{C_{0corr}} - 1\right)L^3\right]^{\frac{1}{3}} \quad (3)$$

where C_{0corr} and C_{corr} are given by,

$$C_{0corr} = C_{ini} - \frac{3L}{5GA} \quad (4)$$

$$C_{corr} = C - \frac{3L}{5GA} \quad (5)$$

where C_{ini} is the initial compliance, and C is the instantaneous compliance during loading. Then, G_{II} can be obtained by substituting a with a_{eq} in Eq. 2.

Material Properties

The PSB components were manufactured using 4-year-old *Phyllostachys*, a common bamboo genus cultivated in southeast China. Mechanical properties of PSB composite evaluated in this study have been determined in previous work, and the elastic

parameters are presented in Table 1 (Huang *et al*. 2015a), where E is Young's modulus, G is the shear modulus, and u is Poisson's ratio. The x-axis is the direction parallel to the strands, *i.e*., the longitudinal direction of PSB, and the y-axis and z-axis are the other two transverse directions perpendicular to the x-axis.

Table 1. Elastic Parameters of PSB Composite Used in This Study

E_x (MPa)	E_y (MPa)	E_z (MPa)	u_{xy}	u_{yx}	G_{xy} (MPa)	G_{xz} (MPa)	G_{yz} (MPa)
11890	3066	3066	0.077	0.300	1446	1446	746

ENF Tests

The sizes of ENF specimens should be chosen carefully. The following two factors should be taken into consideration:

First, seeking to reduce the influence of shear deformation, when the span-to-depth ratio of the specimen satisfies $2L/2h>10$, the influence of shearing force becomes very small and can be neglected (Yoshihara 2003).

Second, crack propagation occurs before flexural failure. Assuming that all regions are in the elastic state except the crack tip, then, if $a \leq 0.5L$, the mid-span ($x=L$) will be the most prone to flexural failure, the half depth of the cross section should be satisfied $h \geq \frac{4EG_{\mathrm{IIc}}L^2}{\sigma^2 a^2}$; else if $0.5L<a<L$, the layered section ($x=a$) will be the most prone to flexural failure, the half depth of the cross section should be satisfied $h \geq \frac{4EG_{\mathrm{IIc}}}{\sigma^2}$. where σ is the bending strength of the PSB composite.

Referring to the G_{IIc} values of most wood produces and glued wood materials (Kretschmann 2010), an ENF specimen with dimensions of 450 mm (L, parallel to strands) × 40 mm (h, perpendicular to strands) × 20 mm (b, perpendicular to strands) was designed, as shown in Fig. 2. In total, 6 categories with 5 specimens each were tested, with crack lengths changed from 75 mm to 185 mm to investigate the influence of crack length on G_{IIc} (Table 2).

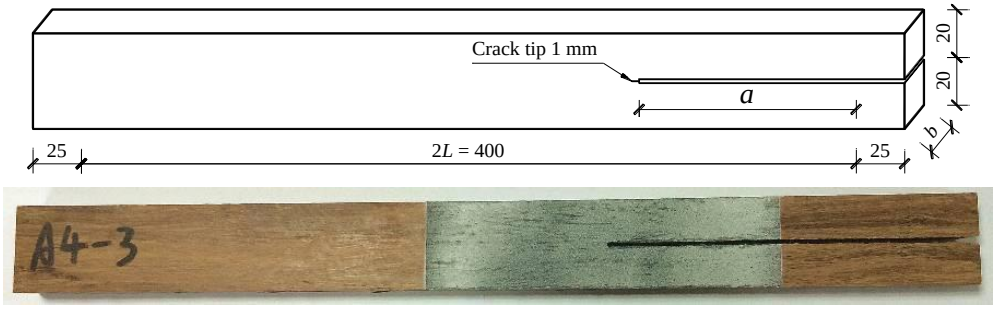

Fig. 2. ENF specimen (measurements in mm)

The through-width crack was first cut to length a along the longitudinal direction by a band saw with 1.5 mm thickness, and then it was extended by 1 mm at the tip using a razor blade. Two sheets of light gauge steel coated with lubricating oil were inserted between the crack surfaces to reduce the friction between the upper and lower cantilever beams. The beam had a span of 400 mm, and each support was located at 25 mm from

the closet end of the specimen. A vertical downward load was applied at mid-span at a speed of 2 mm/min. The load point displacement was measured with a telescopic displacement meter, and the strain field around the crack tip was measured using digital image correlation (DIC). To increase the accuracy of DIC, speckle paint was sprayed on the specimen around the crack tip to increase the recognition of the test specimen surface.

Table 2. Dimensions and Crack Lengths of ENF Specimens

Category	Span $2L$ (mm)	Depth $2h$ (mm)	Width b (mm)	Crack Length a (mm)	Crack-Span Ratio a/L	Numbers
A1	400	40	20	75	0.375	5
A2				100	0.500	5
A3				125	0.625	5
A4				155	0.775	5
A5				170	0.850	5
A6				185	0.925	5

RESULTS AND DISCUSSION

Fracture Processes

It is difficult to measure the crack propagation length during fracture due to the concealment of the crack opening, but the development of superficial shear strain around crack tip can be recorded by DIC. For example, Fig. 3 shows the behavior of the specimen labeled A4 during the loading process. The crack extended along the longitudinal direction, which was parallel to the initial crack direction. The crack propagation of mode II fracture of PSB was self-similar cracking when the crack was parallel to the strand. Stress concentration around the crack tip can be observed. The range of stress concentration at point B was wider than that at point A due to the development of the fracture process zone (FPZ) (Vasic and Smith 2002; Morel *et al*. 2005). The compliance in the load-displacement curve increased at point A, which indicated the initiation of the development of the FPZ. The development of the FPZ caused a non-negligible amount of energy dissipation, containing the crack tip deformation, nonlinear behavior of the material, root additional rotation, thereby enhanced the fracture toughness.

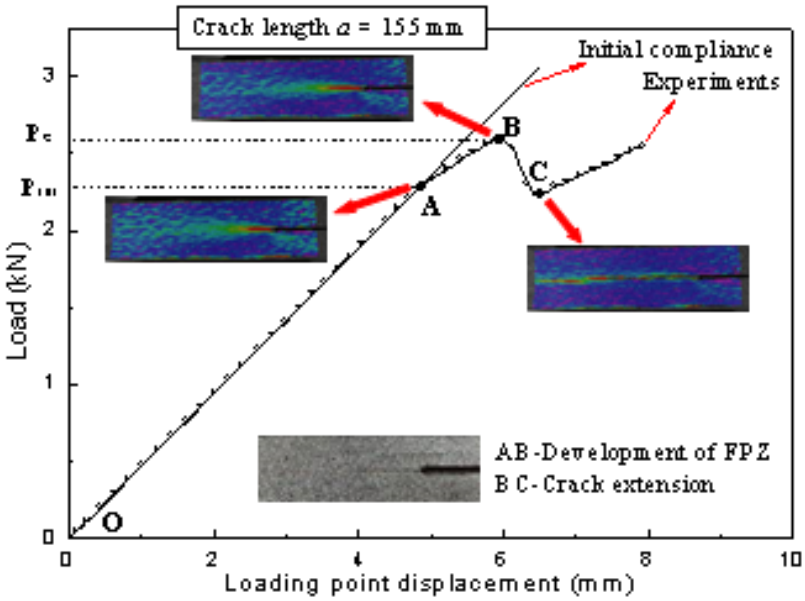

Fig. 3. Loading process of the specimen labeled A4

Figure 4 shows the typical load-displacement curves of each group. The crack growth was unstable if $a < 0.7\ L$, while it was stable if $a > 0.7\ L$ (Boyano *et al*. 2017). For the specimens with a = 75 mm, 100 mm, or 125 mm, after crack initiation the applied load exhibited a significant decline as the crack rapidly propagated to a certain level, corresponding to snap-back instability (Carpinteri 1989). For the specimens with a = 155 mm, 170 mm, or 185 mm, the crack was relatively hard to extend due to the friction between the delaminated parts of the specimen in the neighborhood of the loading roller and the lock effect of transverse load at the mid-span, which increased the influence of the FPZ and produced a pseudo toughening effect (Fan *et al*. 2007).

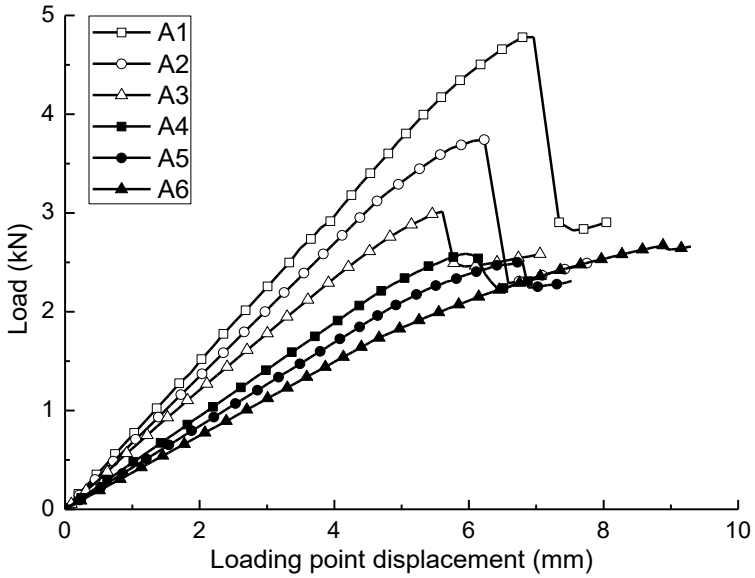

Fig. 4. Load-displacement curves

FPZ Length and Crack Propagation Length

The equivalent crack length, a_{eq}, can be calculated by substituting the instantaneous compliance into Eq. 3. Hence, before crack propagation, the length of the FPZ can be calculated as $\Delta a_{FPZ} = a_{eq}-a$. After crack propagation, the crack extension length can be calculated as $\Delta a=a_{eq}-\Delta a_{FPZ}^{max}$.

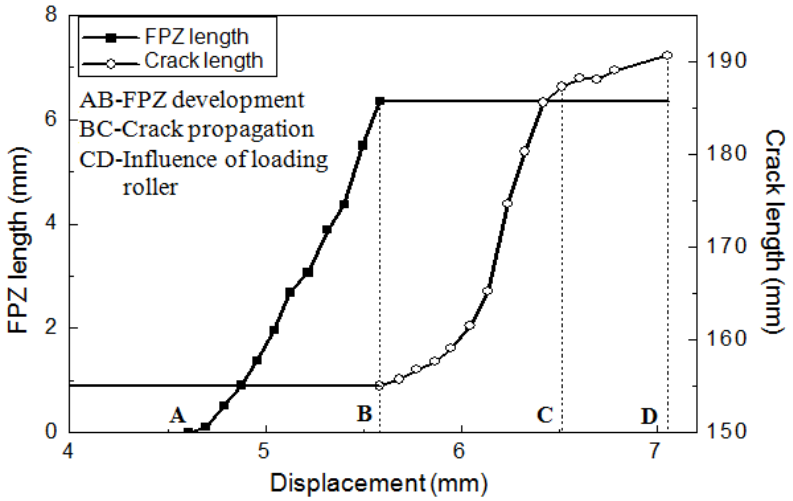

Fig. 5. FPZ length and crack propagation length of the specimen labeled A4

Taking the specimen with an initial crack length of 155 mm as an example, the development of the FPZ and crack length are described in Fig. 5. Points A, B, and C were consistent with the relevant points in Fig. 3. Softening onset was at point A, and the length of the FPZ increased until point B. Then, cracking initiated at point B and extended to a length of about 185 mm within the range of BC. Subsequently, the crack was hard to propagate due to the stress concentration caused by the loading roller.

R-curves and Critical Energy Release Rate G_{IIc}

The fracture behavior of composite materials is commonly evaluated by the resistance curve (R-curve), which is the relation between the energy release rate and crack propagation length. An approach to determine the R-curve is to evaluate the energy release rate from the load-displacement curve using the CBBM; G_{II} of every moment during fracture can be calculated through Eq. 2 by replacing a with a_{eq}. A sample R-curve obtained by this method is presented in Fig. 6. The beginning of the curve increased with equivalent crack growth, which indicated that the energy was used to drive the FPZ development. The mean value of the initial energy release rate, G_{IIini}, corresponding to the onset of FPZ development, was calculated as 1.65 N/mm. Then, the crack began to expand after the development of the FPZ. The curve became approximately horizontal during crack propagation. The suggested value of the critical energy release rate, G_{IIc}, corresponding to the initiation of crack extension, was calculated as 2.57 N/mm. In the third section, the curve increases due to the influence of the loading roller. Therefore, G_{II} can be considered constant during crack extension.

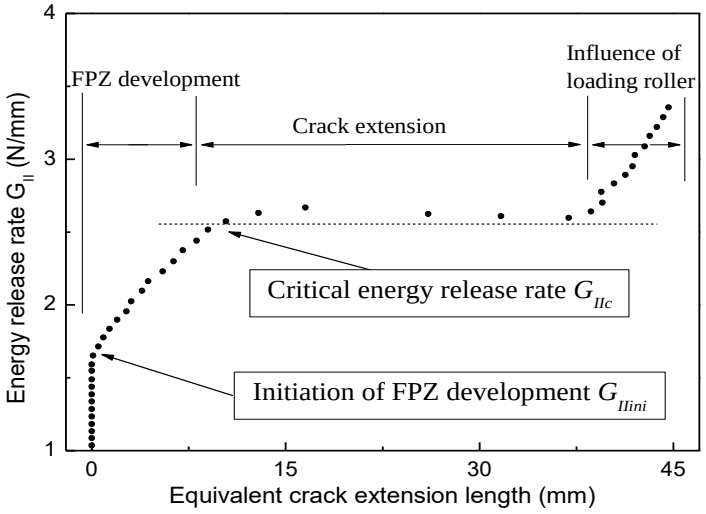

Fig. 6. R-curve of the specimen labeled A4

The relationship between G_{IIc} and a_0 obtained from CBBM is shown in Fig. 7. The results reveal that the values of G_{IIc} for each group with different crack lengths are almost the same. The mode II fracture critical energy release rate of PSB is a constant independent of the initial crack length, and the mean value of G_{IIc} was 2.61 N/mm.

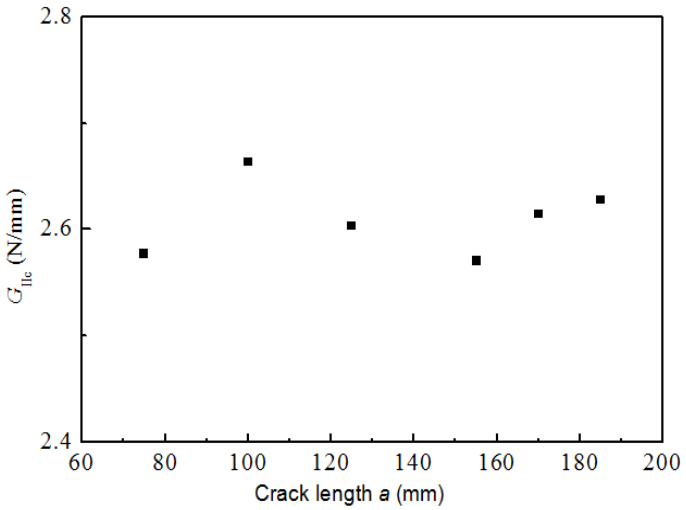

Fig. 7. Critical energy release rate *vs*. initial crack length

Fracture Toughness K_{IIc}

From the theory of linear elastic fracture mechanics, if the plasticity near the crack tip can be neglected, the energy release rate G and the stress intensity factor K are identical for isotropic materials (Rice 1968). Sih *et al*. (1965) derived the analytical solutions for the near-tip stress in orthotropic composites using complex variable functions. It was verified that the relation between elastic stress and energy during crack propagation in isotropic bodies can be extended to those in anisotropic bodies. The energy release rate G_{II} can be transformed into the stress intensity factor K_{II} by the following equation,

$$K_{\mathrm{II}} = \sqrt{\frac{E_{\mathrm{x}} G_{\mathrm{II}}}{\alpha_{\mathrm{II}}}} \tag{6}$$

where

$$\alpha_{\mathrm{II}} = \frac{1}{\sqrt{2}} \sqrt{\sqrt{\frac{E_{\mathrm{x}}}{E_{\mathrm{y}}}} + \frac{1}{2}\left(\frac{E_{\mathrm{x}}}{G_{\mathrm{xy}}} - 2\mu_{\mathrm{xy}}\right)} \tag{7}$$

where μ_{xy} is the Poisson's ratio for deformation along the *y*-axis caused by stress along the *x*-axis.

For ENF tests, by substituting the elastic parameters of PSB and the expression of G_{II} into Eq. 6, the stress intensity factor K_{II} is derived as follows:

$$K_{\mathrm{II}} = \frac{P}{b\sqrt{2h}}\left(1.5813\frac{a}{2h} + 0.3906\right) \tag{8}$$

It is shown that the value of K_{II} is simply determined by the specimen configuration, crack length, and applied load. Fracture toughness K_{IIc} is the value of K_{II} at crack initiation. The mean value of K_{IIc} was calculated as 4436 kN·m$^{-3/2}$ through Eq. 8 by replacing P with P_{c}. Table 3 compares mode II fracture toughness among selected timber species and PSB composite. The result reveals that K_{IIc} in PSB composite is much greater than in commonly used timber products.

Table 3. Comparison of K_{IIc} among Selected Species and PSB

Species	K_{IIc} (kN·m$^{-3/2}$)	
	TL	RL
Douglas-fir		2230
Western hemlock	2240	----
Scots pine	2050	----
Southern pine	2070	----
Red spruce	2190	1665
Poplar	----	2232[a]
PSB composite	4436	

* Unless otherwise stated, values are taken from the *Wood Handbook* (Kretschmann 2010); where *L* is parallel to the grain in which the crack propagates, *R* is perpendicular to the grain but normal to the growth rings, and *T* is perpendicular to the grain but tangent to the growth rings;
[a] Xu *et al*. (1996)

CONCLUSIONS

1. The mode II fracture of PSB composite is self-similar cracking when the crack runs parallel to the strands. The fracture process contains two stages: the development of the FPZ and the crack propagation stage. The development of the FPZ enhances the fracture toughness by causing a non-negligible amount of energy dissipation before crack propagation. Cracking initiates when the FPZ length increases to the maximum value.
2. The critical energy release rate G_{IIc} was calculated by CBBM. The mean value of G_{IIc}

of PSB was 2.61 N/mm independent of the initial crack length.

3. The R-curve shows a gradual increase with increasing equivalent crack length, which indicates that the energy is used to drive the FPZ development, then becomes approximately horizontal during crack propagation. Without considering the possible influence of the loading roller, it can be thought that G_{II} is a constant during crack extension.
4. The mean value of the critical stress intensity factor K_{IIc} of PSB was 4436 $kN \cdot m^{-3/2}$, which is much greater than those of commonly used timber products.

ACKNOWLEDGMENTS

The authors are grateful for the support of the National Science Fund of China (No.51778299), the Priority Academic Program Development of Jiangsu Higher Education Institutions, and the Doctorate Fellowship Foundation of Nanjing Forestry University.

REFERENCES CITED

ASTM D2344 (2016). "Standard test method for short-beam strength of polymer matrix composite materials and their laminates," ASTM International, West Conshohocken, PA, 2016, USA.

ASTM D7905 (2014). "Standard test method for determination of the mode II interlaminar fracture toughness of unidirectional fiber-reinforced polymer matrix composites," ASTM International, West Conshohocken, PA, 2014, USA.

Barrett, J. D., and Foschi, R. O. (1977). "Mode II stress-intensity factors for cracked wood beams," *Engineering Fracture Mechanics* 9(2), 371-378. DOI: 10.1016/0013-7944(77)90029-7

Boyano, A., De Gracia, J., Arrese, A., and Mujika, F. (2017). "Equivalent energy release rate and crack stability in the End Notched Flexure with inserted roller mixed mode I/II test," *Theoretical and Applied Fracture Mechanics* 87, 99-109. DOI: 10.1016/j.tafmec.2016.11.001

Carlsson, L. A., Gillespie, J. W., and Pipes, R. B. (1986). "On the analysis and design of the end notched flexure (ENF) specimen for mode II testing," *Journal of Composite Materials* 20(6), 594-604. DOI: 10.1177/002199838602000606

Corleto, C. R., and Hogan, H. A. (1995). "Energy release rates for the ENF specimen using a beam on an elastic foundation," *Journal of Composite Materials* 29(11), 1420-1436. DOI: 10.1177/002199839502901101

Carpinteri, A. (1989). "Softening and snap-back instability in cohesive solids," *International Journal for Numerical Methods in Engineering* 28(7), 1521-1537. DOI: 10.1002/nme.1620280705

De Moura, M. F. S. F., Campilho, R. D. S. G., and Gonçalves, J. P. M. (2009). "Pure mode II fracture characterization of composite bonded joints," *International Journal of Solids and Structures* 46(6), 1589-1595. DOI: 10.1016/j.ijsolstr.2008.12.001

De Moura, M. F. S. F., Silva, M. A. L., De Morais, A. B., and Morais, J. J. L. (2006). "Equivalent crack based mode II fracture characterization of wood," *Engineering Fracture Mechanics* 73(8), 978-993. DOI: 10.1016/j.engfracmech.2006.01.004

Fan, C., Jar, P.-Y. B., and Cheng, J. J. R. (2007). "A unified approach to quantify the role of friction in beam-type specimens for the measurement of mode II delamination resistance of fibre-reinforced polymers," *Composites Science and Technology* 67(6), 989-995. DOI: 10.1016/j.compscitech.2006.06.011

Griffith, A. A. (1921). "The phenomena of rupture and flow in solids," *Philosophical Transactions of the Royal Society A* 221(582-593), 163-198. DOI: 10.1098/rsta.1921.0006

Huang, D., Bian, Y., Zhou, A., and Sheng, B. (2015a). "Experimental study on stress–strain relationships and failure mechanisms of parallel strand bamboo made from *Phyllostachys*," *Construction and Building Materials* 77, 130-138. DOI: 10.1016/j.conbuildmat.2014.12.012

Huang, D., Bian, Y., Huang, D., Zhou, A., and Sheng, B. (2015b). "An ultimate-state-based-model for inelastic analysis of intermediate slenderness PSB columns under eccentrically compressive load," *Construction and Building Materials* 94, 306-314. DOI: 10.1016/j.conbuildmat.2015.06.059

Huang, D., Zhou, A., and Bian, Y. (2013). "Experimental and analytical study on the nonlinear bending of parallel strand bamboo beams," *Construction and Building Materials* 44(8), 585-592. DOI: 10.1016/j.conbuildmat.2013.03.050

Irwin, G. R. (1956). "Onset of fast crack propagation in high strength steel and aluminum alloys," *Sagamore Research Conference Proceedings* 2, 289-305.

Kretschmann, D. E. (2010). "Mechanical properties of wood," in: *Wood Handbook*, Forest Products Laboratory U.S. Department of Agriculture Forest Service, Madison, WI, USA.

Morel, S., Dourado, N., and Valentin, G. (2005). "Wood: A quasibrittle material R-curve behavior and peak load evaluation," *International Journal of Fracture* 131(4), 385-400. DOI: 10.1007/s10704-004-7513-0

Rice, J. R. (1968). "A path independent integral and the approximate analysis of strain concentration by notches and cracks," *Journal of Applied Mechanics* 35(2), 379-386. DOI: 10.1115/1.3601206

Russell, A. J., and Street, K. N. (1982). "Factors affecting the interlaminar fracture energy of graphite/epoxy laminates," in: *Progress in Science and Engineering of Composites, ICCM-IV*, T. Hayashi, K. Kawata, and S. Umekawa (eds.), Tokyo, Japan, pp. 279-286.

Sih, G. C., Paris, P. C., and Irwin, G. R. (1965). "On cracks in rectilinearly anisotropic bodies," *International Journal of Fracture Mechanics* 1(3), 189-203. DOI: 10.1007/BF00186854

Valvo, P.S. (2018). "The effects of shear on Mode II delamination: A critical review," *Frattura ed Integrita Strutturale* 12(44), 123-139. DOI:10.3221/IGF-ESIS.44.10

Vasic, S., and Smith, I. (2002). "Bridging crack model for fracture of spruce," *Engineering Fracture Mechanics* 69(6), 745-760. DOI: 10.1016/S0013-7944(01)00091-1

Wang, Y., and Williams, J. G. (1992). "Corrections for mode II fracture toughness specimens of composites materials," *Composites Science and Technology* 43(3), 251-256. DOI: 10.1016/0266-3538(92)90096-L

Wang, H., and Vu Khanh, T. (1996). "Use of end-loaded-split (ELS) test to study stable fracture behaviour of composites under mode II loading," *Composite Structures* 36(1), 71-79.

Williams, J. G., and Hadavinia, H. (2002). "Analytical solutions for cohesive zone models," *Journal of the Mechanics and Physics of Solids* 50(4), 809-825. DOI: 10.1016/S0022-5096(01)00095-3

Xu, S., Reinhardt, H. W., and Gappoev, M. (1996). "Mode II fracture testing method for highly orthotropic materials like wood," *International Journal of Fracture* 75(3), 185-214. DOI: 10.1007/BF00037082

Yoshihara, H. (2003). "Resistance curve for the mode II fracture toughness of wood obtained by the end-notched flexure test under the constant loading point displacement condition," *Journal of Wood Science* 49(3), 210-215. DOI: 10.1007/s10086-002-0467-9

Article submitted: October 11, 2018; Peer review completed: December 31, 2018; Revised version received and accepted: January 3, 2019; Published: January 10, 2019.
DOI: 10.15376/biores.14.1.1579-1590